



The energy implication of climate change on urban wastewater systems

Masoumeh Khalkhali, Weiwei Mo^{*}

Department of Civil and Environmental Engineering, University of New Hampshire, USA

ARTICLE INFO

Article history:

Received 9 October 2019
Received in revised form
20 April 2020
Accepted 24 April 2020
Available online 18 May 2020

Handling Editor: Prof. Jiri Jaromir Klemes

Keywords:

Water-energy nexus
Urban wastewater treatment plant
Embodied energy
Energy recovery and offset
Climate change
Sustainability of wastewater treatment

ABSTRACT

Urban wastewater service provision is an important energy consumer as well as a potentially important energy producer. This study aims to advance understandings on the influence of climate change on the intra- and inter-annual patterns of wastewater treatment plants' net life cycle energy consumption. Historic monthly operational data of a wastewater treatment plant in the northeast United States were obtained and its current net life cycle energy demand was investigated. Comprehensive multivariate and multiple linear regression analyses were then performed. The main climate variables (temperature, rainfall, and snowfall) and the wastewater characteristics (flow rate, water temperature, total suspended solids, 5-day biochemical oxygen demand, and chemical oxygen demand) were used to develop regression models for energy that is directly and indirectly consumed and generated at the treatment plant. Two different approaches, a lumped and a month-based method, for conducting the regression analysis were investigated. Whenever possible, these two approaches were combined to improve the predictive power of the regression models. The obtained result shows the treatment plant's direct energy use consists of more than 86% of the total energy consumption currently. Various energy recovery strategies allow the treatment plant to offset more than 15% of its total energy consumption. The future annual wastewater influent of the plant was projected to decrease towards the end of the century under climate change, with a significantly larger seasonal variation. The influent wastewater quality is projected to decrease, leading to higher direct and indirect energy consumption for treatment. Projections of future intra-annual responses show that the seasonal variations of wastewater flowrate as well as the monthly cumulative energy demand can potentially experience a two-fold increase, resulting in more frequent system shocks and create operational difficulties.

© 2020 Elsevier Ltd. All rights reserved.

1. Introduction

Wastewater treatment plants (WWTPs) are important energy users in the US, representing around 24% of a typical municipality's energy budget (Edward III, 2004) and around 0.6% of the nation's total energy consumption (Soares et al., 2017). Energy used in WWTPs contributes to 46.4 million metric tons/year of greenhouse gas emissions in the US (Griffiths-Sattenspiel and Wilson, 2009), in addition to the small but indispensable amounts of greenhouse gases that are directly released during the treatment processes (Zhao et al., 2019). Furthermore, a comparable amount of energy is indirectly consumed throughout the supply chain of the materials/

chemicals used in WWTPs (Mo and Zhang, 2012). WWTPs are also important energy producers, via means such as combined heat and power (CHP) generation utilizing biogas produced through sludge digestion (Mo and Zhang, 2013), hydropower generation harnessing the kinetic energy embedded in wastewater flow (Power et al., 2014), and residual heat recovery from wastewater (Suzuki et al., 2009). The energy recovery potential of CHP has been estimated to range from 0.4 to 1.5 times of a WWTP's operational energy (Bachmann et al., 2015; Diaz-Elsayed et al., 2019; Gu et al., 2017; Nouri et al., 2006; Wett et al., 2007). Wastewater hydropower generation potential has been estimated to be around 0.75% of WWTPs' operational energy use in the UK on average (Power et al., 2014), while in certain cases, a full energy offset is possible (Samora et al., 2016). Furthermore, the potential of residual heat recovery has been estimated to offset at least 50% of a WWTP's heating/cooling energy demand (Hao et al., 2015). Both energy consumption (Li et al., 2018) and energy production (Khalkhali et al., 2018) in

^{*} Corresponding author. 35 Colovos Road, 334 Gregg Hall, Durham, NH, 03824, USA.

E-mail address: Weiwei.mo@unh.edu (W. Mo).

WWTPs are subject to future changes in climate. Increase in precipitation frequency and intensity can increase pollutant mobilization (Alamdari et al., 2017), and consequently, the pollution load of combined sewer systems (Santana et al., 2014), which may lead to higher energy consumptions in the wastewater treatment processes. Climate also has a direct effect on operational energy and chemical consumptions through changes in microbial activities (Wilén et al., 2006) and/or chemical reaction rates (Mines et al., 2007). Changes in runoff volume and temperature can also directly influence hydropower generation, the efficiency of residual heat recovery (Chae and Ren, 2016), and the effectiveness of biogas generation (Bowen et al., 2014). Nevertheless, our understandings of the trend and the magnitude of such influences to inform sustainable WWTP management remain limited.

Efforts have been previously made to quantify the influence of climate change on wastewater quantity (Ma et al., 2014) and quality (Wang et al., 2017) at WWTPs. These studies commonly use process-based models or statistical methods. Process-based models take a mechanistic approach to characterize the physical, chemical, or biological processes in the WWTPs. For instance, Semadeni-Davies et al. (2008) simulated stormwater and sewer infiltration through hydrological and hydrodynamical models to explore the effect of climate change on the volume of urban drainage (Semadeni-Davies et al., 2008). Jin et al. (2016) combined a runoff routing model and a process-based activated sludge model to predict wastewater quantity and quality under heavy rainfall events (Jin et al., 2016). While process-based models are useful in laying the theoretical foundation of the relationships between climate and wastewater quantity and quality, they can be limited in dealing with complex WWTP treatment processes where the underlying mechanisms are less understood. To address this issue, statistical methods have been applied. Carstensen et al. (1998) found that a simple regression model based on measured data performed significantly better than a complex hydrological model in predicting a WWTP's hydraulic load (Carstensen et al., 1998). Langeveld et al. (2014) adopted an empirical approach to study the diurnal dynamics of wastewater composition in relation to climate and predicted the chemical oxygen demand and the ammonium concentrations of the influent wastewater (Langeveld et al., 2014). Wang et al. (2017) analyzed the influence of cold and warm seasons on a Norwegian WWTP using correlation analysis and showed that snow melting has a significant impact on the quantity and quality of wastewater influent in cold climate area (Wang et al., 2017). None of these studies, however, further linked climate's influence to the embedded energy of wastewater treatment.

During the last decade, there has also been a proliferation of life cycle assessment (LCA) studies investigating both energy consumptions and productions from WWTPs considering construction, operation, and end-of-life stages (Mo et al., 2011). These LCAs often include a system boundary of upstream processes (wastewater collection and transport to the plant) (Lassaux et al., 2007), core processes (treatment processes in the plant) (Tangsubkul et al., 2006), and downstream processes (the production of by-products such as electricity/heat by biogas or the residuals and their recycling) (Mo and Zhang, 2012). Functional units based upon unit volume of wastewater being treated have been commonly adopted. Previously reported net life cycle energy use in WWTPs ranged from 0.09 to 1.37 kWh/m³ (Bodik and Kubaska, 2013; CEC, 2005; McCarty et al., 2011; Mo and Zhang, 2012; Plappally, 2012; Silvestre et al., 2015; Stillwell et al., 2010; Wang, H. et al., 2016; Wilkinson, 2000). While these LCAs offer important insights into WWTPs' life cycle energy compositions, they are mostly static analyses based upon temporally averaged inventory data, which cannot be easily extrapolated to investigate potential future changes under climate change. Only a few studies have examined the dynamic

relationship between climate and the life cycle energy of water or wastewater systems. Santana et al. (2014) adopted a linear regression analysis combined with relative importance analysis to determine the influence of water quality on the embodied energy of a drinking water treatment plant. They found that the influent water quality variation can cause up to 14.5% variation in total operational embodied energy, mainly due to different treatment chemical dosage requirement (Santana et al., 2014). Mo et al. (2016) and Stang et al. (2018) combined multivariate, regression, and relative importance analyses to investigate the influence of climate and water quality changes on the energy and chemical consumptions in drinking water supply. They found future climate change can either increase or decrease the life cycle energy of water supply depending on geographic locations and treatment processes (Mo et al., 2016; Stang et al., 2018). Li et al. (2018) is by far the only study that investigated the influence of rainfall changes on the life cycle energy demand of WWTPs through comprehensive correlation and regression analyses. They found a positive relationship between rainfall and the studied WWTP's environmental impacts, including global warming, acidification, and photochemical ozone creation. However, future climate scenarios were not used in their prediction of the WWTPs' dependence on energy.

Accordingly, this study aims to develop a generalizable modeling and assessment framework to investigate the influence of climate change on WWTPs' life cycle energy consumption and recovery, considering a system boundary that includes the upstream, core, and downstream processes. This modeling and assessment framework includes a correlation analysis between climate and raw wastewater quantity and quality indicators, as well as regression and relative importance analyses that further link climate and wastewater quantity and quality indicators with the life cycle energy consumption and recovery at the WWTPs. The modeling framework was then applied to a WWTP located in Boston, MA. This study allows generation of new knowledge and understandings in the following areas: 1) the influence of future climate change on raw wastewater quantity and quality, 2) the influence of climate on future changes in the volumetric and total energy consumption (direct and indirect) and generation towards the end of the century, and 3) the influence of climate change on the seasonal energy consumption (direct and indirect) and generation patterns.

2. Methods

This study adopted life cycle assessment as a framework to inventory the historic WWTP direct and indirect energy consumptions and energy recoveries. The influence of climate change on the energy use and generation at the WWTPs was then quantified through integrated correlation, regression, and relative importance analyses as described in detail in the following sub-sections.

2.1. Study site description

Deer Island wastewater treatment plant (DIWWTP), located in Boston, Massachusetts, owned and operated by the Massachusetts Water Resources Authority, is the second largest WWTP in the US. It provides wastewater treatment services to 2.2 million people (32% of the state population) in 43 communities (1350 km² service area) of the greater Boston area. Around 93% of its service area is served by separate sanitary and stormwater systems, while 7% is served by combined sewers. However, only about half of the annual flow treated at the DIWWTP is sanitary flow, with the remaining flow being groundwater infiltration and stormwater inflow (I/I) entering the separated sewer system, as well as stormwater from combined sewers (MWRA, 2013). The average daily flow to the plant is 1.36

million m³ and the plant has a peak wet weather capacity of 4.81 million m³ per day. The plant employs a treatment process that consists of primary and secondary treatment, followed by disinfection and dechlorination. The detailed treatment process and chemicals applied are outlined in Fig. 1. The types of energy directly used onsite are electricity and diesel. Electricity is primarily used for wastewater pumping and treatment as well as for administrative and support activities. Diesel is used as a backup power supply. Additionally, sludge is treated for phosphorous removal, thickened, and anaerobically digested. The biogas is combusted in a CHP system onsite to offset the plant's electricity and heating demand. The digested sludge is pumped to a residual pellet plant, where it is processed into fertilizer pellets. However, given the residual pellet plant is a separate entity beyond the DIWWTP, production of the fertilizer pellets in the pellet plant was not included in the system boundary of the current study.

Six electric power sources are currently available for the DIWWTP: grid electricity, the electricity recovered from the CHP system, diesel electricity generation (as backup), onsite hydropower generation, onsite wind turbines, and onsite solar photovoltaic arrays. The CHP system consists of two steam turbine generators (STG) of 18 and 1.2-MW power, respectively. The backup power system consists two combustion turbine generators (CTGs) with a capacity of 52 MW. However, diesel electricity generation was not included in the current study due to the intermittent and uncertain nature of its usages. The amount of energy provided by diesel is also insignificant as compared to the total operational energy consumption (2.5%). The hydropower facility generates electricity from the treated wastewater prior to discharge into effluent outfall tunnel using two 1.1-MW Kaplan hydroelectric turbine generators. The onsite wind and solar electricity generations are also not included in this study because they are not directly linked with wastewater characteristics.

In this study, historic monthly precipitation, wastewater quantity and quality, treatment chemical use, and energy use and generation data were directly obtained from the DIWWTP, supplemented by temperature and snowfall data from the National Climate Data Center for Station USW00014739 in Boston, MA (NOAA, 2017). Table 1 shows a summary of the data that have been used by this study.

2.2. Life cycle energy estimation

Life cycle energy was calculated using Eqs. (1) and (2) in this study. It includes three components: 1) direct energy, which includes all types of energy that is directly used onsite of the WWTPs; 2) indirect energy, which includes the energy embodied in the supply chain of the chemicals used during the operation of the WWTPs; and 3) energy offset, which includes energy that is recovered through the CHP system (through steam turbine generation) and the onsite hydropower generation. The present study focuses on the operation stage of the WWTPs because the construction and end-of-life phases of the WWTPs are less relevant to climate change (Mo et al., 2016).

$$VCED_t = VCED_{direct} + VCED_{indirect} - VCED_{offset} \\ = \sum_i PE_i \times E_i + \sum_j PE_j \times E_j - \sum_k PE_k \times E_k \quad (1)$$

$$CED_t = VCED_t \times Q_t \quad (2)$$

Where,

$VCED$ = volumetric cumulative energy demand of wastewater services in month t , MJ/m³;

E = volumetric energy use/chemical use/energy offset in wastewater services, (MJ or ml or g)/m³;

PE = primary energy content, as listed in Table 2, MJ of primary energy; i = energy use index for items listed under "Energy use" in Table 1;

j = chemical species index for items listed under "Chemical use" in Table 1;

k = energy offset index for items listed under "Energy offset" in Table 1;

CED_t = cumulative energy demand of wastewater services in month t , MJ; and

Q_t = total volume of the influent wastewater during month t , m³.

The Ecoinvent 3 and the USLCI databases embedded in the SimaPro software (version 9.0.033) and the "Cumulative Energy Demand V1.09" method were utilized to calculate the life cycle energy of the DIWWTP (Jassal et al., 2013). A list of the data entries

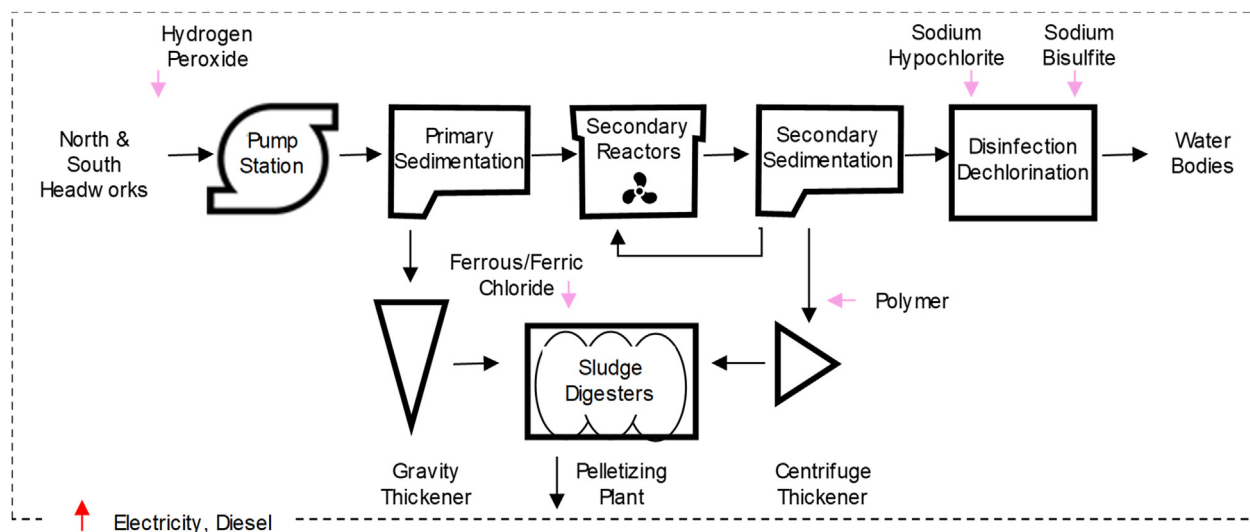


Fig. 1. The treatment process and the chemicals used in the Deer Island Wastewater Treatment Plant.

Table 1

Annual variations in climate, wastewater characteristics, energy consumption, and energy offset of the Deer Island Wastewater Treatment Plant.

Data item		Time period	Minimum monthly value	Average monthly value	Maximum monthly value	Usage/Application
Climate	Temperature (°C)	Jul 2000–Apr 2017	−7.17	11.09	25.17	N.A.
	Precipitation (m)	Jul 2000–Apr 2017	0.02	0.09	0.38	
	Snowfall (m)	Jul 2000–Apr 2017	0.00	0.12	1.65	
Wastewater characteristics	Influent flowrate (m ³ /s)	Jul 2000–Apr 2017	9.40	14.61	31.79	N.A.
	Water temperature (°C)	Jan 2007–Oct 2017	12.71	17.52	22.97	
	pH	Jan 2007–Oct 2017	6.31	6.64	6.85	
	TSS (mg/L)	Jul 2006–Aug 2018	89.42	183.72	281.55	
	BOD ₅ (mg/L)	Jul 2006–Aug 2018	83.22	172.89	269.66	
	COD (mg/L)	Jan 2010–Aug 2018	173.79	391.97	551.47	
Chemical use	Hydrogen peroxide (mL/m ³)	Jul 2004–Apr 2017	0.00	1.70	11.94	Pretreatment & Odor control
	Sodium hypochlorite (mL/m ³)	Jul 2004–Apr 2017	5.62	12.11	22.00	Disinfection
	Sodium bisulfite (mL/m ³)	Jul 2004–Apr 2017	0.00	0.93	1.52	Dechlorination
	Ferrous/Ferric chloride (g/m ³)	Jul 2004–Apr 2017	0.44	1.48	3.20	Control the formation of struvite and reduce H ₂ S in biogas for emission control
Energy use	Polymer (g/m ³)	Jul 2004–Apr 2017	0.02	0.15	0.35	Used for sludge thickening
	Support facilities (MJ/m ³)	Jul 2006–Apr 2017	0.03	0.07	0.11	Office, laboratory, maintenance shops and warehouse, including a small-scale replica of the plant secondary treatment to test and compare a variety of biological and physical treatment processes on a large scale before those processes become part of the full-scale facility.
	Pumping (MJ/m ³)	Jul 2006–Apr 2017	0.31	0.34	0.37	Used for lifting collected urban wastewater to the head of the plant (46 m)
	Primary treatment (MJ/m ³)	Jul 2006–Apr 2017	0.08	0.16	0.25	Used for non-suspended solids settlement
	Secondary treatment (MJ/m ³)	Jul 2006–Apr 2017	0.18	0.37	0.61	Used for onsite oxygen generation for pure oxygen-activated sludge system and non-settleable solids removal through biological and gravity treatment
	Residual processing (MJ/m ³)	Jul 2006–Apr 2017	0.07	0.19	0.31	Used for sludge thickening of primary and secondary sludge, pumping of sludge and anaerobic digestion of sludge.
	Thermal plant (MJ/m ³)	Jul 2006–Apr 2017	0.04	0.10	0.15	Used for thermal energy production for processes and facility heating and power generation
	Steam turbine generation (MJ/m ³)	Jul 2006–Apr 2017	0.76	2.17	3.15	Electricity generated from steam produced from utilization of methane gas generated from sludge digestion in boilers
	Methane gas (MJ/m ³)	Jul 2003–Apr 2015	0.00	1.89	3.36	Byproduct of sludge digestion
	Hydropower (MJ/m ³)	Jul 2006–Apr 2017	0.00	0.04	0.06	Used for heating and power generation
						Generated from the effluent water of the plant

Table 2

Data entries in SimaPro corresponding to each type of energy implication and their unit primary energy content.

	Chemical/energy types	SimaPro entries	Unit primary energy content (MJ)
Direct energy use	Electricity (MJ)	Electricity, at eGrid, NEWE, 2010/kWh/RNA	2.26
Indirect energy use	Hydrogen Peroxide (mL)	Hydrogen peroxide, without water, in 50% solution state (GLO) market for Alloc Def, U	0.03
	Sodium hypochlorite (mL)	Sodium hypochlorite, without water, in 15% solution state (GLO) market for Alloc Def, U	0.02
	Bisulfite (mL)	Sodium hydrogen sulfite (GLO) market for Alloc Def, U	0.05
	Polymer (g)	Cationic resin (GLO) market for Alloc Def, U	0.04
	Ferrous/Ferric Chloride (g)	Iron (III) chloride, without water, in 40% solution state (GLO) market for Alloc Def, U	0.02
Energy offset	Steam turbine generator (MJ)	Electricity, at eGrid, NEWE, 2010/kWh/RNA	2.26
	Hydropower (MJ)	Electricity, at eGrid, NEWE, 2010/kWh/RNA	2.26

used in SimaPro is provided in Table 2. Steam turbine and hydro-power generation was assumed to replace electricity supply from the grid.

2.3. Multivariate and multi-linear regression analyses

Multivariate and multi-linear regression analyses were conducted to model the climate's influence on the influent wastewater characteristics as well as the required treatment. A multivariate analysis and a Principal Component Analysis (PCA) was first conducted using the JMP Pro 14.2.0® software to investigate the correlations among three monthly climate indicators (mean temperature (T_{mean}), total snowfall amount (S_{total}), and total rainfall amount (P_{total})) and six wastewater indicators (pH, mean wastewater temperature (T_w), total suspended solids (TSS), five-day biochemical oxygen demand (BOD_5), chemical oxygen demand (COD), average influent wastewater rate (Q_{avg})). Strength of the pairwise correlations were evaluated using the Pearson correlation coefficients (r) which has a value between +1 and -1, where +1 indicates total positive linear correlation; 0 indicates no linear correlation; and -1 indicates total negative linear correlation (Stigler, 1989). In this study, r values in ranges of [0.7–1], [0.5–0.7], [0.2–0.5], and (0–0.2) are considered to indicate strong, moderate, fair, and weak correlations, respectively (Akoglu, 2018). While no two variables are entirely “independent” from a statistical perspective, extremely high collinearity ($r > 0.99$) could mean that the variables essentially represent the same information. Information redundancy can result in over-inflated variances, making the following regression analysis inaccurate. Data availability, causal relationships, and prior knowledge of the processes being modeled are used to eliminate redundant variables and select the most appropriate predictor. It has to be noted that T_{mean} was selected as the only temperature indicator in this study because a previous study has found extremely high collinearity among mean, maximum, and minimum monthly temperatures in Boston ($r > 0.99$) (Mo et al., 2016).

Comprehensive regression analyses were then performed to predict climate's influence on the operation of the DIWWTP. A regression analysis was first conducted to investigate the influence of climate indicators on influent wastewater quantity. Both climate and wastewater quantity indicators were then used to predict wastewater quality. Lastly, all climate and wastewater quality indicators were used to predict direct and indirect energy consumptions as well as the energy offset of wastewater treatment. The regression analyses were also performed in the JMP Pro 14.2.0® software. The stepwise methods (both backward elimination and forward selection algorithms) using both minimum AICc (Akaike Information Criterion) and BIC (Bayesian Information Criterion) stopping rules were adopted and the highest obtained adjusted R squared (R^2_{adj}) values were reported. The R^2_{adj} value compares the descriptive power of regression models. It is a modified version of

R^2 that has been adjusted for the number of predictors in the model (Wherry, 1931). The R^2_{adj} increases only if the newly added predictive variable improves the model more than would be expected by chance. The R^2_{adj} value is normally between 0 and 1. A higher R^2_{adj} indicates that the model has a stronger predictive power. In this study, models with a R^2_{adj} value higher than 0.5 (50% of variation of the response is explainable by the independent predictors) were used for future predictions.

Two approaches were tested for conducting the regression analysis: 1) a lumped approach and 2) a month-based approach. The lumped approach uses all available monthly data for the regression analysis. The lumped dataset does not differentiate inter- and intra-annual changes. In other words, both the inter- and the intra-annual changes in the climate are used as a surrogate to predict the influence of future climate change on the operation of the DIWWTP. The month-based approach performs a regression analysis for each of the twelve months. Inter-annual changes are hence separated from intra-annual changes and only intra-annual changes are used to predict future operation of the DIWWTP. This approach, however, significantly reduces the amount of data that can be used for each regression. In this study, when sufficient data are available, a mixed approach was adopted, which determines whether the lumped or the month-based approach would be used to maximize the R^2_{adj} values for each month. Overall, the mixed approach was found to be more suitable for wastewater quantity predictions, while the lumped approach was found to be more suitable for predicting wastewater quality as well as chemical and energy consumptions due to lack of data availability.

The relative importance of each predictor was then calculated using the standardized regression coefficients, also labeled as Standard Betas (Bring, 1994). Standardized regression coefficients are the average changes of the dependent variables in response to one-unit change of a predictor, when other predictors are held constant. The variance inflation factor (VIF) is used to assess multicollinearity of the selected regression models, which further indicates the degree to which the precision of the model (R^2_{adj}) is degraded by multicollinearity (James et al., 2013). VIF values of less than 10 have been previously considered to show that collinearity problems are negligible or non-existent (Marquardt, 1970), while VIF values of greater than 100 have been considered to indicate significant multicollinearity (O'Brien, 2007). The same criteria are adopted to evaluate the multicollinearity of the regression models reported in this study.

2.4. Climate change scenarios

Downscaled climate model outputs including monthly average temperature and precipitation were obtained from the Bureau of Reclamation for 21 General Circulation Models (GCMs) from the CMIP5 archive. The 21 models, listed in Tables S–1, have been statistically downscaled to 1/8th degree resolution over the

continental United States using the Bias-Correction and Spatial Disaggregation technique (Wood et al., 2002). Two Representative Concentration Pathways were used for future predictions, one representing a low/medium emission scenario (RCP 4.5) and one representing a high emission scenario (RCP 8.5). These scenarios are consistent with a wide range of possible changes in future anthropogenic greenhouse gas emissions and have been widely adopted by previous studies (Daniel et al., 2018). Emissions in the RCP 4.5 scenario peak around 2040, then decline, while in the RCP 8.5 scenario, emissions continue to rise throughout the 21st century (Collins et al., 2013). Snowfall amount under climate change scenarios is assumed to be proportional to the amount of precipitation being projected under these scenarios.

3. Results and discussion

In this section, historic life cycle energy consumption and generation, correlations between water quality/climate indicators and energy consumption and generation, as well as the future inter- and intra-annual energy use trends of the WWTP are reported.

3.1. Average monthly life cycle energy of the DIWWTP

Fig. 2 shows the average monthly influent wastewater volume, the average monthly volumetric cumulative energy demand (VCED), and the total monthly cumulative energy demand (CED) of the DIWWTP for the period of 2007–2017. The average monthly influent wastewater volume peaks in March and then drops to its lowest value in September (a 63% reduction compared to March) before rising again in winter. The high raw wastewater volume in March could be contributed by a combined effect of higher rainfall volume, melting snowpack, and lower stormwater infiltration and evapotranspiration. On the other hand, the low raw wastewater volume in September can be contributed by the combined effect of lower rainfall volume, lower groundwater table, and higher stormwater infiltration and evapotranspiration. It has to be noted that the rate of drinking water supply in the same region is the highest in July and August and the lowest in February. This indicates a weak correlation between drinking water supply and wastewater generation in the region ($r = -0.4$).

In terms of the VCED, direct energy represents around 86–92% of the monthly energy consumption, which is much more significant than the indirect energy. Secondary treatment (30%) and pumping (27%) are the two largest components of the volumetric

direct energy use, followed by residual processing (16%), primary treatment (13%), thermal plant (8%), and support of the system (6%). Volumetric direct energy consumption is the highest in August–September and the lowest in March–April, which is mainly resulted from changes in secondary treatment and residual processing (Figure S-1 in the supporting information). The mixed nature of urban runoff and sewage in the DIWWTP can play a significant role in creating this pattern. During spring, sewage is diluted by snow melt and hence is lower in pollutant concentrations, resulting in a lower treatment need. Temperature also has a significant impact on the dissolved oxygen (DO) of wastewater and the need for aeration and mixing (Marx et al., 2010). Temperature has a positive relationship with biological activity and its associated DO consumption (Dugan et al., 2009). In addition, warmer water has a lower DO holding capacity (Dugan et al., 2009; Lekov et al., 2009). Collectively, these effects increase the volumetric direct energy consumption in summer, especially the energy used for secondary treatment in which cryogenic and aeration facilities are typically the main energy consumers (McCarty et al., 2011). This aligns with previously reported findings that the energy intensity of secondary treatment is relatively higher at higher temperatures (Bowen et al., 2014). The total direct CED presents a different pattern than the direct VCED. Total direct CED consumption is relatively stable over the year with the highest direct CED occurring in March and the lowest in February. The relatively small variances over the year (17% difference between months with highest and lowest direct CEDs) can be explained by the opposite seasonal trends in the wastewater flow rate and the direct VCED.

Indirect VCED represents around 9–14% of the monthly volumetric energy consumption depending on the month. It shares a similar seasonal pattern as the direct VCED (Figure S-2 in the supporting information). This is because more chemicals are needed in summer to treat the same volume of wastewater due to a lower wastewater quality in summer months. Sodium hypochlorite has the highest contribution to the volumetric indirect energy use, representing 65% of the average indirect energy use intensity. Hydrogen peroxide has an average annual contribution of 14% in indirect energy intensity. This is closely followed by sodium bisulfite (13% of the indirect energy intensity), and the rest of the chemicals together contribute around 8% of the indirect energy intensity. Hydrogen peroxide is only applied in summer for odor control. This is because when increased DO demand is not sufficiently satisfied by increased aeration, dead spots will be created where concentrations of ammonia, phosphates, or sulfur

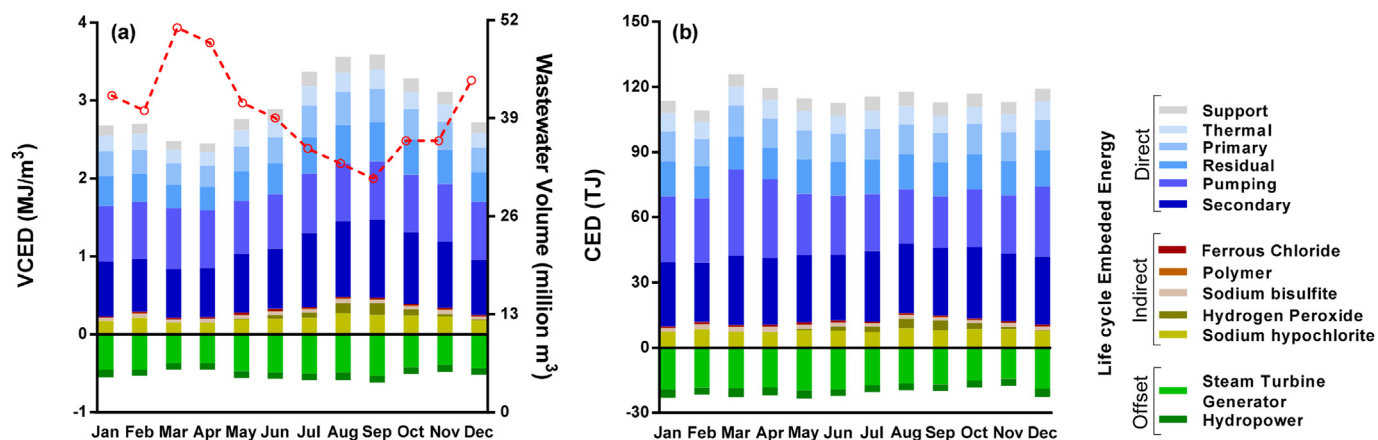


Fig. 2. The embodied energy of DIWWTP in three groups of direct, indirect and energy offset. (a) the monthly volumetric cumulative energy demand (VCED) to treat 1 m³ of wastewater in stacked bars as well as the average monthly influent wastewater rate in red dashed line; and (b) the monthly cumulative energy demand (CED) in stacked bars. (For interpretation of the references to colour in this figure legend, the reader is referred to the Web version of this article.)

compounds will increase. When combined with the monthly wastewater flow rate, indirect CED still peaks in August, although to a lesser extent. January presents the lowest indirect CED, which is 47% below the level of consumption in August.

Volumetric energy offset is around 15–20% of the volumetric energy consumption in the DIWWTP. Energy offset is mostly achieved through steam turbine generation. Volumetric generation of the STG is the lowest in March and April – the snow melting season, which can be explained by the relatively high hydraulic load and low temperature during these months. One thing needs to be noted is that volumetric energy offset from biogas recovery is not the highest in months with the highest organic loadings. Optimal efficiency of anaerobic digestion is achieved under a delicate balance among several groups of microorganisms (Henze et al., 2008). However, this balance can be interrupted by organic shock during the months with the highest organic loadings, resulting in reduction of methane productions (Ketheesan and Stuckey, 2015). This aligns with findings from many previous WWTP behavioral studies that there is an optimal organic loading to achieve the highest efficiency of methane gas productions (Orhoro et al., 2018).

Hydropower generation from the effluent water, with a much smaller contribution to energy offset, does not show significant seasonality due to its dependence to both the effluent flow rate and the tidal elevation variation of the downstream water body. The total CED offset has a slight peak in May and an evident drop in August and September. This drop is primarily resulted from the lower inflow rates in these months.

When energy consumption and recovery are combined, net CED consumption is the highest in August and the lowest in April.

3.2. Multivariate and multiple linear regression analyses

This sub-section reports outcomes related to the correlations between water quality/climate indicators and energy consumption and generation, as well as the future trends of the wastewater treatment demand.

3.2.1. Multivariate correlation analysis

Multivariate correlation analysis was conducted on a dataset consisting of 83 historic months with available information about climate, wastewater, and operation of the plant. The obtained Pearson correlation coefficients (r) for all the existing pairs in this correlation analysis are provided in Fig. 3. There is no extremely high correlation ($r > 0.99$) between climate and wastewater indicator variables. Hence, all variables were kept for the following regression analysis. This is also supported by results obtained from the PCA, which are provided in Tables S–3 of the supporting information.

Average influent wastewater flow rate (Q_{avg}) has a moderate positive correlation with total rainfall P_{total} ($r = 0.61$), a fair negative correlation with mean temperature T_{mean} ($r = -0.40$), and a very weak positive correlation with snowfall S_{total} ($r = 0.09$). The positive correlation between P_{total} and Q_{avg} can be explained by the fact that half of the treated wastewater in this plant is from groundwater infiltration and stormwater inflow. A similar high correlation between P_{total} and Q_{avg} in WWTPs has been reported in Li et al. (2018). A higher T_{mean} reduces soil moisture and hence groundwater infiltration and inflow into the wastewater collection system. Wastewater temperature (T_w) presents a strong similarity to T_{mean} in terms of its correlation with other indicators, except that it has stronger positive correlations with other water quality indicators than T_{mean} . pH is the only wastewater quality indicator that has very weak correlations with climate indicators ($|r| < 0.2$). It has a fair negative correlation with Q_{avg} , which might be explained by the dilution effect of stormwater on raw sewage, which usually has a higher pH than drinking water due to detergents and soap. There are strong correlations between wastewater quality indicators of BOD₅, COD, and TSS, which is expected based upon their definition (Abdalla and Hammam, 2014). TSS, BOD, and COD also present a strong similarity in their correlations with Q_{avg} and climate indicators. They all have a strong negative correlation with Q_{avg} ($r < -0.75$), a fair negative correlation with P_{total} ($r < -0.39$), a fair positive correlation with T_{mean} ($r > 0.24$), and a very weak negative correlation with S_{total} ($r < -0.09$). Negative correlations with Q_{avg} and P_{total} can be explained by the dilution effect of rainfall and increase in I/I which result in less TSS, BOD, and COD, while the positive correlation with T_{mean} can be explained by the higher pollutant loadings found during the summer months.

3.2.2. Regression analysis for wastewater quantity and quality

A multi-linear regression analysis was first performed to examine how climate indicators contribute to the variations of wastewater quantity and quality indicators. The lumped approach was first used for the regression analysis. The obtained results show that Q_{avg} obtained from the lumped approach was not able to replicate the peak flows in March as well as during October and November (Figure S-4 in the SI). The month-based approach was then investigated, which was found to have higher R^2_{adj} values than the lumped approach for seven out of the twelve months (Table 3 and Tables S–3 of the SI). Thus, the mixed approach was adopted for Q_{avg} modeling. Based on the obtained relative importance of the climate variables, P_{total} is the main variable in explaining the Q_{avg} variation for all months except for October. It is the only selected predictor of Q_{avg} in March, which is the month with peak flow. In October, snowfall is possible in the study region and it is the only

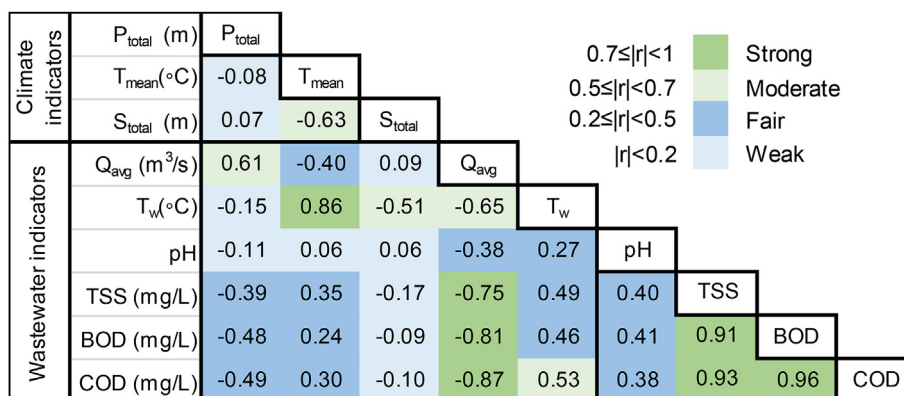


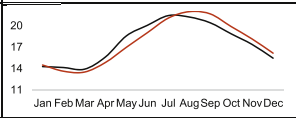
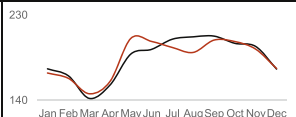
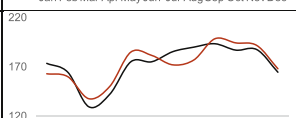
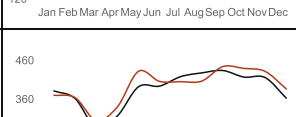
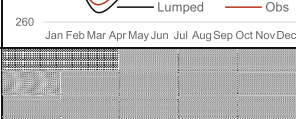
Fig. 3. Pearson correlations coefficient among wastewater and climate indicators.

Table 3
Regression analyses result used for wastewater influent flow rate modeling through Mixed approach.

Month/Method	Jan/Lumped approach					Feb/Lumped approach					Mar/Month-based approach				
	$R^2_{adj} = 0.54$ method = AICc, BIC					$R^2_{adj} = 0.54$ method = AICc, BIC					$R^2_{adj} = 0.71$ method = AICc, BIC				
	Co	S	p	RI (%)	VIF	Co	S	p	RI (%)	VIF	Co	S	p	RI (%)	VIF
Intercept	13.708	0.508	<.0001			13.197	0.201	<.0001			13.680	1.067	<.0001		
P_{total} (m)	43.873	3.477	<.0001	49	1.012	52.322	2.06	0.002	64	1.190	51.236	8.180	<.0001	100	
S_{total} (m)	-2.447	0.993	0.015	12	1.637	-3.006	0.324	0.056	36	1.190					
T_{mean} (°C)	-0.208	0.027	<.0001	39	1.623										
Month/Method	Apr/Lumped approach					May/Month-based approach					Jun/Month-based approach				
	$R^2_{adj} = 0.54$ method = AICc, BIC					$R^2_{adj} = 0.77$ method = AICc, BIC					$R^2_{adj} = 0.69$ method = AICc, BIC				
	Co	S	p	RI (%)	VIF	Co	S	p	RI (%)	VIF	Co	S	p	RI (%)	VIF
Intercept	13.708	0.508	<.0001			19.365	4.747	0.001			9.929	1.016	<.0001		
P_{total} (m)	43.873	3.477	<.0001	49	1.012	37.036	6.741	0.000	77	1.138	46.841	7.926	<.0001	100	1.000
S_{total} (m)	-2.447	0.993	0.015	12	1.637										
T_{mean} (°C)	-0.208	0.027	<.0001	39	1.623	-0.495	0.301	0.125	23	1.138					
Month/Method	July/Lumped approach					Aug/Month-based approach					Sep/Month-based approach				
	$R^2_{adj} = 0.54$ method = AICc, BIC					$R^2_{adj} = 0.58$ method = AICc, BIC					$R^2_{adj} = 0.56$ method = AICc, BIC				
	Co	S	p	RI (%)	VIF	Co	S	p	RI (%)	VIF	Co	S	p	RI (%)	VIF
Intercept	13.708	0.508	<.0001			21.919	6.189	0.003			9.714	0.607	<.0001		
P_{total} (m)	43.873	3.477	<.0001	49	1.012	28.160	6.239	0.001	70	1.000	31.312	6.808	0.000	100	
S_{total} (m)	-2.447	0.993	0.015	12	1.637										
T_{mean} (°C)	-0.208	0.027	<.0001	39	1.623	-0.517	0.269	0.075	30	1.000					
Month/Method	Oct/Month-based approach					Nov/Month-based approach					Dec/Lumped approach				
	$R^2_{adj} = 0.88$ method = AICc, BIC					$R^2_{adj} = 0.59$ method = AICc, BIC					$R^2_{adj} = 0.54$ method = AICc, BIC				
	Co	S	p	RI (%)	VIF	Co	S	p	RI (%)	VIF	Co	S	p	RI (%)	VIF
Intercept	22.377	3.150	<.0001			4.686	2.505	0.082			13.708	0.508	<.0001		
P_{total} (m)						56.433	12.301	0.000	69	1.001	43.873	3.477	<.0001	49	1.012
S_{total} (m)	335.300	30.416	<.0001	78	1						-2.447	0.993	0.015	12	1.637
T_{mean} (°C)	-0.791	0.247	0.007	22	1	0.606	0.295	0.059	31	1.001	-0.208	0.027	<.0001	39	1.623

“Co”: coefficients in linear regression model, “S”: standard errors of the coefficients, “p”: the observed significance level of each predictor variable, “RI”: relative importance of each selected predictor variable in each type of chemical or energy uses calculate based on Standard Betas, “VIF”: variance inflation factor.

Table 4
Regression analyses results for modeling wastewater quality indicators.

Response	R^2_{adj} method	Par.	Int.	P_{total} (m)	S_{total} (m)	T_{mean} (°C)	Q_{avg} (m³/s)	Modeled (black) vs. observed (red)
T_w (°C)	0.74 AICc	Co	20.727	14.705	-0.791	0.210	-0.464	
		Sd	0.613	2.606	0.529	0.017	0.040	
		p	<.0001	<.0001	0.138	<.0001	<.0001	
		RI (%)		17	4	41	38	
		VIF		1.810	1.825	2.343	2.260	
TSS (mg/L)	0.64 AICc	Co	299.068	92.780	-15.255		-8.379	
		Sd	8.230	49.767	8.092		0.669	
		p	<.0001	0.059	0.058		<.0001	
		RI (%)		12	9		79	
		VIF		1.586	1.025		1.604	
BOD (mg/L)	0.70 AICc, BIC	Co	309.507			-0.525	-9.037	
		Sd	9.469			0.210	0.554	
		p	<.0001			0.014	<.0001	
		RI (%)				13	87	
		VIF				1.255	1.255	
COD (mg/L)	0.74 AICc	Co	684.062			-0.749	-20.051	
		Sd	22.722			0.496	1.385	
		p	<.0001			0.135	<.0001	
		RI (%)				9	91	
		VIF				1.232	1.232	
pH	0.19 AICc	Co	6.869	0.435			-0.019	
		Sd	0.045	0.270			0.004	
		p	<.0001	0.110			<.0001	
		RI (%)	0.000	24			76	
		VIF		1.585			1.585	

month that Q_{avg} is positively and significantly affected by S_{total} , probably due to rain-on-snow events. For the remaining months with lower temperature, precipitation mainly happens in the form of snow and due to decrease in rainfall, a decrease in Q_{avg} in December, January, and February is expected. T_{mean} generally has weak and negative influence on Q_{avg} in most months, due to its impact on evaporation and soil moisture.

The lumped approach was selected for examining the contributions of climate and wastewater flowrate to wastewater quality changes, as the data availability ($n = 7$) limited the use of the month-based approach. The regression analysis yielded acceptable prediction models for all wastewater quality parameters except for pH. Both T_{mean} and Q_{avg} were found to be statistically significant contributors to T_w variations (Table 4). Q_{avg} was found to be a very significant contributor to TSS, BOD, and COD predictions. Other predictor variables present limited contributions to the wastewater quality indicators.

3.2.3. Future wastewater treatment demand

Regression analysis was then performed to examine the contribution of both climate and wastewater quality indicators to the volumetric chemical and energy uses of the DIWWTP. The obtained results are provided in Table 5. Out of the direct energy consumption models, electricity use for pumping is the only response variable that did not yield an acceptable prediction model ($R^2_{adj} < 0.50$). This is expected as pumping energy intensity is primarily determined by pumping efficiency, which is not expected to present a significant seasonal pattern. The remaining direct electricity uses are all well explainable by climate and wastewater indicators ($R^2_{adj} > 0.79$). COD is the most frequently selected predictor for different types of direct energy uses, followed by T_w , TSS, T_{mean} , P_{total} , S_{total} , and pH. Out of the chemical response variables, ferrous/ferric chloride and sodium bisulfite are the two response variables that did not result in satisfactory regression models. This can be explained by the expected higher uncertainty related to processes where these chemicals are used: struvite control in anaerobic digestion and dichlorination, respectively. Sodium hypochlorite, hydrogen peroxide, and polymer resulted in satisfactory predictive models ($R^2_{adj} > 0.52$). Sodium hypochlorite usage can be predicted by pH, COD, and T_w , as less sodium hypochlorite is needed with lower pH, higher pollution concentration is and lower water temperature. Hydrogen peroxide usage increases with higher wastewater temperature, higher pH, and lower P_{total} . It enhances oxidation as due to temperature rise and decrease in solubility of oxygen, mechanical aeration will not be sufficient to increase the DO during hot summer months. Polymer use in secondary treatment can be predicted by BOD, COD, T_w and P_{total} . In terms of energy offset, the analyses did not result in an acceptable predictive model for energy offset through the steam turbine generator (STG) ($R^2_{adj} = 0.44$). Methane gas generated from sludge digestion in this system is the primary fuel for the STG. Further analysis shows that an acceptable model can be obtained for the volumetric methane gas production ($R^2_{adj} = 0.77$) with TSS, BOD₅ and COD selected as predictors. The difference between the R^2_{adj} values of the STG and the methane gas models can be explained by the seasonal changes in the turbine generation and waste heat recovery efficiencies, which cancels out the effect of seasonal water quality changes. No satisfactory model was found for volumetric hydropower generation.

3.3. Future trend of DIWWTP's embodied energy under climate change

Fig. 4 provides the predicted future trend of wastewater generation and life cycle energy of the DIWWTP under RCP 4.5 and RCP

8.5 climate change scenarios. The response variables that were not found to be correlated with climate data in the previous step were assumed constant under climate change. Q_{avg} has shown an overall decreasing trend towards the end of the century under both climate scenarios (Fig. 4(a)). Temperature increase plays a dominant role in the decrease of Q_{avg} . Under RCP 4.5, the estimated Q_{avg} for the late-century period is slightly higher than the mid-century period. This is because under this scenario, carbon emissions peak in 2040 and as a result, temperature increase slows down toward the late-century.

Direct and indirect VCEDs are expected to increase by 2.7–3.3% and 6.4–7.9% under RCP 4.5 and 8.5 scenarios, respectively. This increasing trend in direct and indirect VCEDs can be linked to the decrease in Q_{avg} and its influence on wastewater quality. Volumetric energy offset presents a relatively stable or slightly decreasing trend towards the late century, although temperature and organic concentrations are expected to be higher. This could again be the result of potential shocks in organic loadings and the limitations in maximum achievable efficiency in energy recovery. Total monthly CED of the DIWWTP is projected to increase by 2 and 6% under the RCP 4.5 and 8.5 scenarios, respectively. Both direct and indirect CEDs were projected to increase by around 1.7–2.3% and 3.9–5.3% towards the end of the century under climate change, while offset CED was projected to drop by 1–2%. The DIWWTP has been looking into combining food waste with sludge digestion to increase biogas recovery.

3.4. Future seasonality of the embodied energy under climate change condition

Fig. 5 presents the estimated seasonal variation in Q_{avg} , VCED, and CED at the late-century period under RCP 4.5 (black) and RCP 8.5 (red) scenarios. Q_{avg} is projected to maintain a seasonal pattern with peaks in March and drops in late summer and early fall. However, a larger seasonal variation in Q_{avg} is observed under both scenarios. Differences between the highest and lowest flow rates within a year are going to increase from 63% in the baseline period to as much as 121% in the late-century period. This is also evidenced in the standard deviation of Q_{avg} , which increases from 2.39 m³/s in the baseline period to 2.75–3.57 m³/s in the late-century period under the two climate scenarios. These changes can potentially result in more frequent system shocks with extremely high and low flow rates, and hence create operational difficulties. The VCED of the plant will experience a relatively consistent increasing trend through the year. October will experience the highest increase in VCED from the baseline for 0.23 and 0.53 MJ/m³ under RCP 4.5 and 8.5 scenarios, respectively. November will experience decrease in VCED compared to the baseline due to slight rise in the region's precipitation in this month and its dilution effect on water quality. Projections of future intra-annual CED changes show that the plant will experience a significantly larger seasonal variation of CED between June and November. Differences between the highest and lowest month CEDs within the timeframe increased from 19% in the baseline period to as much as 39% in the late-century period.

4. Conclusions and implications

In this study, the future trends of intra- and inter-annual life cycle energy consumption and generation under climate change is explored, using the Deer Island Wastewater Treatment Plant as a testbed. Currently, direct energy contributes more than 86% to the total Cumulative Energy Demand (CED) consumption, while energy recovery through Combined Heat and Power and hydropower generation allows the treatment plant to offset more than 15% of its energy demand. A multivariate analysis based upon historical data

Table 5
Regression analyses coefficients for modeling wastewater indirect/direct energy use and energy offset.

Response	R _{adj} ² method	Par.	Int.	P _{total} (m)	S _{total} (m)	T _{mean} (°C)	T _w (°C)	pH	TSS (mg/L)	BOD ₅ (mg/L)	COD (mg/L)
Electricity use for Pumping (MJ/m ³)	0.39 AICc, BIC	Co	0.4465	0.0884			0.0016	−0.0212	−0.0003	0.0003	
		Sd	0.0555	0.0257			0.0004	0.0087	0.0001	0.0001	
		p	<.0001	0.0009			<.0001	0.0169	0.0003	0.0010	
		RI (%)	13				17	9	31	29	
		VIF	1.2675				1.2922	1.2074	5.7458	6.2367	
Electricity use in Primary Treatment (MJ/m ³)	0.87 AICc	Co	−0.0275	−0.2056		−0.0015	0.0093		−0.0002		0.0003
		Sd	0.0145	0.0388		0.0004	0.0012		0.0001		0.0001
		p	0.0607	<.0001		0.0002	<.0001		0.0556		0.0002
		RI (%)	11			17	37		10		25
		VIF	1.4927			6.2340	7.6258		9.4987		12.9490
Electricity use in Secondary Treatment (MJ/m ³)	0.89 AICc	Co	−0.0307	−0.1684		0.0124			−0.0013		0.0011
		Sd	0.0237	0.0678		0.0012			0.0002		0.0001
		p	0.1984	0.0152		<.0001			<.0001		<.0001
		RI (%)	5			22			26		47
		VIF	1.4092			1.4271			7.5958		9.1851
Electricity use in Residual Processing (MJ/m ³)	0.84 AICc, BIC	Co	−0.4200	−0.2292	0.0287		0.0075	0.0589	−0.0004		0.0005
		Sd	0.1197	0.0589	0.0103		0.0010	0.0189	0.0002		0.0001
		p	0.0008	0.0002	0.0065		<.0001	0.0026	0.0164		<.0001
		RI (%)	10	8			24	7	15		36
		VIF	1.4591	1.8064			2.2877	1.2443	8.3634		10.3316
Electricity use in Thermal Plant (MJ/m ³)	0.79 AICc, BIC	Co	−0.1641	−0.1493	0.0146		0.0031	0.0251			0.0002
		Sd	0.0653	0.0306	0.0053		0.0005	0.0103			0.0000
		p	0.0141	<.0001	0.0072		<.0001	0.0169			<.0001
		RI (%)	19	12			28	9			32
		VIF	1.2837	1.5506			2.1011	1.1980			1.8846
Electricity use for system support (MJ/m ³)	0.86 AICc, BIC	Co	−0.0099	−0.0586	0.0118	0.0005	0.0025		−0.0002		0.0002
		Sd	0.0077	0.0167	0.0035	0.0002	0.0006		0.0001		0.0000
		p	0.2033	0.0008	0.0013	0.0185	0.0001		0.0009		<.0001
		RI (%)	8	8	11	19			19		35
		VIF	1.5056	1.7501	6.2727	7.1283			9.8226		13.6215
Sodium Hypochlorite (mL/m ³)	0.52 AICc, BIC	Co	−71.9216				0.3348	10.8594			0.0160
		Sd	16.1945				0.1096	2.5154			0.0048
		p	<.0001				0.0031	<.0001			0.0012
		RI (%)					29	38			33
		VIF					1.4034	1.1771			1.5250
Hydrogen Peroxide (mL/m ³)	0.64 AICc, BIC	Co	−33.5213	−11.451			0.5964	3.8567			
		Sd	9.5365	4.0725			0.0585	1.4557			
		p	0.0007	0.0062			<.0001	0.0098			
		RI (%)	18				66	17			
		VIF	1.0034				1.0672	1.0644			
Polymer (g/m ³)	0.63 AICc	Co	−0.0979	−0.1492			0.0046			0.0009	0.0001
		Sd	0.0296	0.0867			0.0014			0.0002	0.0000
		p	0.0013	0.0882			0.0018			<.0001	0.0024
		RI (%)	11				21			48	20
		VIF	1.3592				1.3817			2.3104	1.4220
Ferrous & Ferric chloride (g/m ³)	0.28 AICc, BIC	Co	−7.4226	−3.5723	0.6183	0.0292		1.3476			
		Sd	2.8997	1.2530	0.2560	0.0078		0.4349			
		p	0.0124	0.0056	0.0181	0.0003		0.0027			
		RI (%)	22	21	33			24			
		VIF	1.0173	1.7329	1.7110			1.0179			
Sodium bisulfite (mL/m ³)	0.08 AICc	Co	1.6814			0.0067	−0.034			−3.5310	
		Sd	0.2720			0.0037	0.0115			0.00002	
		p	<.0001			0.0795	0.0037			0.1119	
		RI (%)				65	20			15	
		VIF				4.0414	4.5491			1.3203	
Steam turbine electricity generation (MJ/m ³)	0.44 AICc	Co	0.0058	−0.2336	0.0723	0.0027					0.0006
		Sd	0.0499	0.1480	0.0328	0.0011					0.0001
		p	0.9082	0.1186	0.0305	0.0112					<.0001
		RI (%)	13	20	25						42
		VIF	1.3360	1.7119	1.8739						1.4810
Digester Gas Production (L/m ³)	0.77 AICc	Co	17.9468						−0.2975	0.1949	0.2853
		Sd	6.7759						0.0926	0.1294	0.0623
		p	0.0103						0.0021	0.1373	<.0001
		RI (%)							27	17	56
		VIF							6.7183	12.671	14.0483

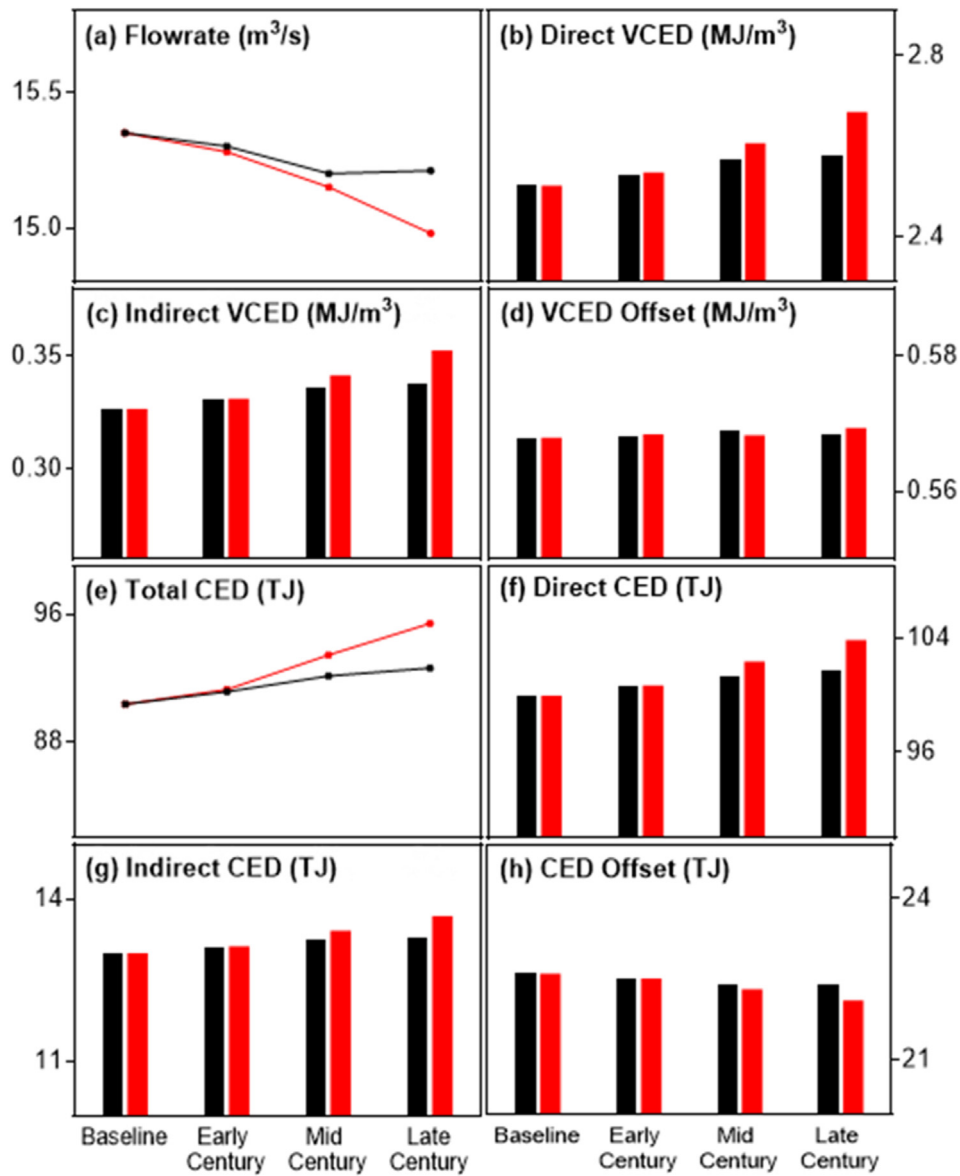


Fig. 4. The future wastewater volume and embodied energy of DIWWTP under climate change scenarios of RCP 4.5 (black) and RCP 8.5 (red). (For interpretation of the references to colour in this figure legend, the reader is referred to the Web version of this article.)

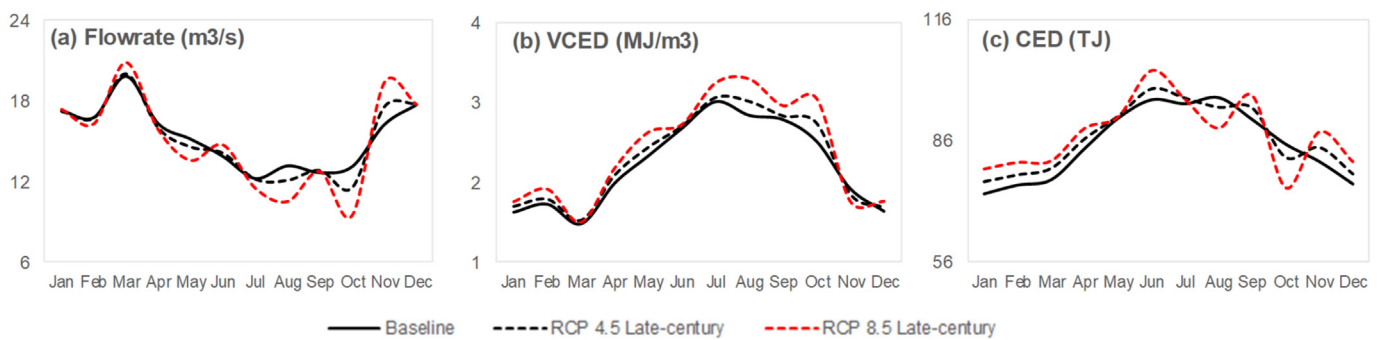


Fig. 5. Comparison of the projected seasonal changes in (a) wastewater flowrate, (b) volumetric cumulative energy demand, and (c) total cumulative energy demand in late-century period under the RCP 4.5 and 8.5 scenarios.

show wastewater quantity and most wastewater quality variables have a strong correlation with climate factors. Most of the energy

and chemical consumption as well as energy offset variables can be predicted by climate and wastewater characteristic parameters.

Two climate scenarios of the RCP 4.5 and RCP 8.5 are investigated. Annual influent wastewater quantity is predicted to decrease towards the end of the century under both climate change scenarios, mainly due to the expected increase in temperature. However, a larger seasonal variation in the flow rate is projected, which might more than double the current seasonal variations in flow rates. This can potentially result in more frequent system shocks with extremely high and low flow rates, and hence challenge the operation of the treatment plant. The influent wastewater quality will also decrease under climate change conditions which implies more direct and indirect energy consumptions for wastewater treatment. Overall, the plant's CED consumption is expected to rise. Direct energy demand will increase more than indirect energy demand. The energy offset potential of the plant is projected to slightly decrease due to potential disturbances to the delicate microbial balance required for efficient biogas recovery in the anaerobic digestion. Projections of future intra-annual responses show that the seasonal variations of wastewater flowrate as well as the monthly cumulative energy demand can potentially experience a two-fold increase, resulting in more frequent system shocks and create operational difficulties. Future study can extend the current work to additional wastewater treatment plants to investigate the influence of treatment system design and geospatial heterogeneity on the outcome as well as allow comparison of various data-driven regression and machine learning models.

Declaration of competing interest

The authors declare that they have no known competing financial interests or personal relationships that could have appeared to influence the work reported in this paper.

CRediT authorship contribution statement

Masoumeh Khalkhali: Data curation, Formal analysis, Methodology, Writing - original draft. **Weiwei Mo:** Conceptualization, Funding acquisition, Methodology, Supervision, Writing - original draft.

Acknowledgement

The authors are grateful for the technical support of Mr. David F. Duest, Director of the Deer Island Wastewater Treatment Plant. The authors would also like to thank Mr. David F. Duest and Mr. Robert Huang for reviewing and providing construction suggestions about the manuscript. The authors would like to acknowledge the support of the National Science Foundation under a CRISP Type I Award (#BCS-1638334) and a CBET Award (#CBET-1706143). Any opinions, findings, and conclusions or recommendations expressed in this material are those of the authors and do not necessarily reflect the views of the National Science Foundation.

Appendix A. Supplementary data

Supplementary data to this article can be found online at <https://doi.org/10.1016/j.jclepro.2020.121905>.

References

Abdalla, K.Z., Hammam, G., 2014. Correlation between biochemical oxygen demand and chemical oxygen demand for various wastewater treatment plants in Egypt to obtain the biodegradability indices. *Int. J. Sci. Basic Appl. Res.* 13 (1), 42–48.

Akoglu, H., 2018. User's guide to correlation coefficients. *Turkish J. Emer. Med.* 18 (3), 91–93.

Alamdari, N., Sample, D.J., Steinberg, P., Ross, A.C., Easton, Z.M., 2017. Assessing the effects of climate change on water quantity and quality in an urban watershed

using a calibrated stormwater model. *Water* 9 (7), 464.

Bachmann, N., la Cour Jansen, J., Bochmann, G., Montpart, N., 2015. Sustainable Biogas Production in Municipal Wastewater Treatment Plants. IEA Bioenergy Massongex, Switzerland.

Bodik, I., Kubaska, M., 2013. Energy and sustainability of operation of a wastewater treatment plant. *Environ. Protect. Eng.* 39 (2), 15–24.

Bowen, E.J., Dolfig, J., Davenport, R.J., Read, F.L., Curtis, T.P., 2014. Low-temperature limitation of bioreactor sludge in anaerobic treatment of domestic wastewater. *Water Sci. Technol.* 69 (5), 1004–1013.

Bring, J., 1994. How to standardize regression coefficients. *Am. Statistician* 48 (3), 209–213.

Carstensen, J., Nielsen, M.K., Strandbæk, H., 1998. Prediction of hydraulic load for urban storm control of a municipal WWT plant. *Water Sci. Technol.* 37 (12), 363–370.

CEC, C.E.C., 2005. California's Water-Energy Relationship Tech. Rep. CEC-700-2005-011-SF. California Energy Commission, Sacramento, CA.

Chae, K.-J., Ren, X., 2016. Flexible and stable heat energy recovery from municipal wastewater treatment plants using a fixed-inverter hybrid heat pump system. *Appl. Energy* 179, 565–574.

Collins, M., Knutti, R., Arblaster, J., Dufresne, J., Fichet, T., Friedlingstein, P., 2013. The New Concentration Driven RCP Scenarios and Their Extensions, pp. 1045–1047. Chap. 12.

Daniel, J.S., Jacobs, J.M., Miller, H., Stoner, A., Crowley, J., Khalkhali, M., Thomas, A., 2018. Climate change: potential impacts on frost–thaw conditions and seasonal load restriction timing for low-volume roadways. *Road Mater. Pavement Des.* 19 (5), 1126–1146.

Diaz-Elsayed, N., Rezaei, N., Guo, T., Mohebbi, S., Zhang, Q., 2019. Wastewater-based resource recovery technologies across scale: a review. *Resour. Conserv. Recycl.* 145, 94–112.

Dugan, N.R., Williams, D.J., Meyer, M., Schneider, R.R., Speth, T.F., Metz, D.H., 2009. The impact of temperature on the performance of anaerobic biological treatment of perchlorate in drinking water. *Water Res.* 43 (7), 1867–1878.

Edward III, G., 2004. Water and Wastewater Industry Energy Efficiency: A Research Roadmap. Awwa Research Foundation.

Griffiths-Sattenspiel, B., Wilson, W., 2009. The Carbon Footprint of Water. River Network, Portland.

Gu, Y., Li, Y., Li, X., Luo, P., Wang, H., Robinson, Z.P., Wang, X., Wu, J., Li, F., 2017. The feasibility and challenges of energy self-sufficient wastewater treatment plants. *Appl. Energy* 204, 1463–1475.

Hao, X., Liu, R., Huang, X., 2015. Evaluation of the potential for operating carbon neutral WWTPs in China. *Water Res.* 87, 424–431.

Henze, M., van Loosdrecht, M.C., Ekama, G.A., Brdjanovic, D., 2008. Biological Wastewater Treatment. IWA publishing.

James, G., Witten, D., Hastie, T., Tibshirani, R., 2013. An Introduction to Statistical Learning. Springer.

Jassal, R.S., Black, T.A., Arevalo, C., Jones, H., Bhatti, J.S., Sidders, D., 2013. Carbon sequestration and water use of a young hybrid poplar plantation in north-central Alberta. *Biomass Bioenergy* 56, 323–333.

Jin, Y., You, X.-y., Ji, M., 2016. Process response of wastewater treatment plant under large rainfall influent flow. *Environ. Eng. Manage. J.* 15 (11).

Ketheesan, B., Stuckey, D.C., 2015. Effects of hydraulic/organic shock/transient loads in anaerobic wastewater treatment: a review. *Crit. Rev. Environ. Sci. Technol.* 45 (24), 2693–2727.

Khalkhali, M., Westphal, K., Mo, W., 2018. The water-energy nexus at water supply and its implications on the integrated water and energy management. *Sci. Total Environ.* 636, 1257–1267.

Langeveld, J., Schilperoord, R., Rombouts, P., Benedetti, L., Amerlinck, Y., de Jonge, J., Flameling, T., Nopens, I., Weijers, S., 2014. A new empirical sewer water quality model for the prediction of WWTP influent quality. In: 13th IWA/IAHR International Conference on Urban Drainage. Sarawak, Malaysia, 7–12 September 2014. Citeseer.

Lassaux, S., Renzoni, R., Germain, A., 2007. Life cycle assessment of water from the pumping station to the wastewater treatment plant. *Int. J. Life Cycle Assess.* 12 (2), 118–126.

Lekov, A., Thompson, L., McKane, A., Song, K., Piette, M.A., 2009. Opportunities for Energy Efficiency and Open Automated Demand Response in Wastewater Treatment Facilities in California—Phase I Report. Lawrence Berkeley National Lab.(LBNL), Berkeley, CA (United States).

Li, Y., Hou, X., Zhang, W., Xiong, W., Wang, L., Zhang, S., Wang, P., Wang, C., 2018. Integration of life cycle assessment and statistical analysis to understand the influence of rainfall on WWTPs with combined sewer systems. *J. Clean. Prod.* 172, 2521–2530.

Ma, S., Zeng, S., Dong, X., Chen, J., Olsson, G., 2014. Short-term prediction of influent flow rate and ammonia concentration in municipal wastewater treatment plants. *Front. Environ. Sci. Eng.* 8 (1), 128–136.

Marquardt, D.W., 1970. Generalized inverses, ridge regression, biased linear estimation, and nonlinear estimation. *Technometrics* 12 (3), 591–612.

Marx, C., Schmidt, M., Flanagan, J., Hanson, G., Nelson, D., Shaw, J., Tomaro, D., Nickels, C., Fass, H., Schmidt, A., 2010. Introduction to Activated Sludge Study Guide. Wisconsin Department of Natural Resources Wastewater Operator Certification.

McCarthy, P.L., Bae, J., Kim, J., 2011. Domestic Wastewater Treatment as a Net Energy Producer—Can This Be Achieved? ACS Publications.

Mines, R.O., Lackey, L.W., Behrend, G.H., 2007. The impact of rainfall on flows and loadings at Georgia's wastewater treatment plants. *Water, Air, Soil Pollut.* 179

- (1), 135–157.
- Mo, W., Wang, H., Jacobs, J.M., 2016. Understanding the influence of climate change on the embodied energy of water supply. *Water Res.* 95, 220–229.
- Mo, W., Zhang, Q., 2012. Can municipal wastewater treatment systems be carbon neutral? *J. Environ. Manag.* 112, 360–367.
- Mo, W., Zhang, Q., 2013. Energy–nutrients–water nexus: integrated resource recovery in municipal wastewater treatment plants. *J. Environ. Manag.* 127, 255–267.
- Mo, W., Zhang, Q., Mihelcic, J.R., Hokanson, D.R., 2011. Embodied energy comparison of surface water and groundwater supply options. *Water Res.* 45 (17), 5577–5586.
- MWRA, 2013. Massachusetts Water Resources Authority (MWRA) Wastewater System Master Plan.
- NOAA, 2017. National climate data center. National oceanic and atmospheric administration. National Climatic Data Center (NCDC). <http://www.ncdc.noaa.gov/oa/ncdc.html>.
- Nouri, J., Jafarinia, M., Naddafi, K., Nabizadeh, R., Mahvi, A., Nouri, N., 2006. Energy recovery from wastewater treatment plant. *Pakistan J. Biol. Sci.* 9 (1), 3–6.
- O'Brien, R.M., 2007. A caution regarding rules of thumb for variance inflation factors. *Qual. Quantity* 41 (5), 673–690.
- Orhorhoro, E.K., Ebunilo, P.O., Sadjere, G.E., 2018. Effect of organic loading rate (OLR) on biogas yield using a single and three-stages continuous anaerobic digestion reactors. *Int. J. Eng. Res. Afr.* 147–155. *Trans Tech Publ.*
- Plappally, A., 2012. Energy requirements for water production, treatment, end use, reclamation, and disposal. *Renew. Sustain. Energy Rev.* 16 (7), 4818–4848.
- Power, C., McNabola, A., Coughlan, P., 2014. Development of an evaluation method for hydropower energy recovery in wastewater treatment plants: case studies in Ireland and the UK. *Sustain. Energy Technol. Assess.* 7, 166–177.
- Samora, I., Manso, P., Franca, M., Schleiss, A., Ramos, H., 2016. Energy recovery using micro-hydropower technology in water supply systems: the case study of the city of Fribourg. *Water* 8 (8), 344.
- Santana, M.V., Zhang, Q., Mihelcic, J.R., 2014. Influence of water quality on the embodied energy of drinking water treatment. *Environ. Sci. Technol.* 48 (5), 3084–3091.
- Semadeni-Davies, A., Hernebring, C., Svensson, G., Gustafsson, L.-G., 2008. The impacts of climate change and urbanisation on drainage in Helsingborg, Sweden: combined sewer system. *J. Hydrol.* 350 (1–2), 100–113.
- Silvestre, G., Fernández, B., Bonmatí, A., 2015. Significance of anaerobic digestion as a source of clean energy in wastewater treatment plants. *Energy Convers. Manag.* 101, 255–262.
- Soares, R.B., Memelli, M.S., Roque, R.P., Gonçalves, R.F., 2017. Comparative analysis of the energy consumption of different wastewater treatment plants. *Int. J. Archit. Arts Appl.* 3 (6), 79.
- Stang, S., Wang, H., Gardner, K.H., Mo, W., 2018. Influences of water quality and climate on the water-energy nexus: a spatial comparison of two water systems. *J. Environ. Manag.* 218, 613–621.
- Stigler, S.M., 1989. Francis Galton's account of the invention of correlation. *Stat. Sci.* 73–79.
- Stillwell, A.S., Hoppock, D.C., Webber, M.E., 2010. Energy recovery from wastewater treatment plants in the United States: a case study of the energy-water nexus. *Sustainability* 2 (4), 945–962.
- Suzuki, H., Dastur, A., Moffatt, S., Yabuki, N., Maruyama, H., 2009. Eco2 cities, ecological cities as economic cities. In: Unedited Conference Edition. The International Bank for Reconstruction and Development/The World Bank, Washington.
- Tangsubkul, N., Parameshwaran, K., Lundie, S., Fane, A., Waite, T., 2006. Environmental life cycle assessment of the microfiltration process. *J. Membr. Sci.* 284 (1–2), 214–226.
- Wang, X., Kvaal, K., Ratnaweera, H., 2017. Characterization of influent wastewater with periodic variation and snow melting effect in cold climate area. *Comput. Chem. Eng.* 106, 202–211.
- Wett, B., Buchauer, K., Fimml, C., 2007. Energy self-sufficiency as a feasible concept for wastewater treatment systems. In: IWA Leading Edge Technology Conference. Singapore: Asian Water, pp. 21–24.
- Wherry, R., 1931. A new formula for predicting the shrinkage of the coefficient of multiple correlation. *Ann. Math. Stat.* 2 (4), 440–457.
- Wilén, B.-M., Lumley, D., Mattsson, A., Mino, T., 2006. Rain events and their effect on effluent quality studied at a full scale activated sludge treatment plant. *Water Sci. Technol.* 54 (10), 201–208.
- Wilkinson, R., 2000. Methodology for Analysis of the Energy Intensity of California's Water Systems and an Assessment of Multiple Potential Benefits through Integrated Water-Energy Efficiency Measures. University of California Santa Barbara.
- Wood, A.W., Maurer, E.P., Kumar, A., Lettenmaier, D.P., 2002. Long-range experimental hydrologic forecasting for the eastern United States. *J. Geophys. Res.: Atmosphere* 107 (D20). ACL 6-1-ACL 6-15.
- Zhao, X., Jin, X., Guo, W., Zhang, C., Shan, Y., Du, M., Tillotson, M., Yang, H., Liao, X., Li, Y., 2019. China's urban methane emissions from municipal wastewater treatment plant. *Earth's Future* 7 (4), 480–490.